An Automatic Travel Control of a Container Crane using Neural Network Predictive PID Control Technique

Jin-Ho Suh[1], Jin-Woo Lee[1], Young-Jin Lee[2] and Kwon-Soon Lee[1,#]

1 Department of Electrical Engineering, Dong-A University, Busan, South Korea
2 Dept. of Electrical Instrument and Control, Korea Aviation Polytechnic College, Kyungnam, South Korea
Corresponding Author / E-mail: kslee@dau.ac.kr, TEL: +82-51-200-7739, FAX: +82-51-200-7743

In this paper, we develop anti-sway control in proposed techniques for an ATC system. The developed algorithm is to build the optimal path of container motion and to calculate an anti-collision path for collision avoidance in its movement to the finial coordinate. Moreover, in order to show the effectiveness in this research, we compared NNP PID controller to be tuning parameters of controller using NN with 2-DOF PID controller. The experimental results for an ATC simulator show that the proposed control scheme guarantees performances, trolley position, sway angle, and settling time in NNP PID controller than other controller. As a result, the application of NNP PID controller is analyzed to have robustness about disturbance which is wind of fixed pattern in the yard.

NOMENCLATURE

XYZ = the fixed coordinate system

$x_T y_T z_T$ = the trolley coordinate system which moves with the trolley

θ = the swing angle of the load in an arbitrary direction in space

(x_m, y_m, z_m) = the position of the load

l = the length of rope

$M_x, M_y, M_l = x, y,$ and l components of the crane mass and the equivalent masses of the rotating parts such as motors and their drive trains

m = the load mass

g = the gravitational acceleration

v_m = the load speed

D_x, D_y, D_l = the viscous damping coefficient associated with $x, y,$ and l motions

f_x, f_y, f_l = the driving forces for the $x, y,$ and l motions

x_S, y_S = start node coordinate value

x_G, y_G = goal node of container coordinate value

x_n, y_n = standard coordinate value of current node

x_t, y_t = contiguity node from current node

x_p, y_p = standard node value

1. Introduction

Recently, the increase of quantity of goods transport is expected by Super Post-Panamax Vessel's appearance. The growth of international container transport has led to increased demand for quay and terminal capacity in ports all over the world. Therefore, necessity of automation of container port handling equipments are risen to reduce of transfer logistics cost and improvement of terminal operation efficiency. Moreover, to accomplish the goal of the program, a highly automated terminal has to be developed. Although, robotizing is not the main goal of the program, it is the opinion that handling containers with a throughput of 500,000TEU a year or more can only be done economically and efficiently by robotizing stacking and terminal transport.

Specially, the project aimed at increasing terminal productivity, both with crane that is divided a system of an AGV and an ASC. Moreover, the improvements in stacking height and efficiency were suggested by using container categories. Terminal productivity is a matter of good and appropriate technical systems on the one hand and the right management on the other hand. In the last decade, we have seen an increase in complexity of the technical systems, especially in the introduction of semi-automated systems. Rotterdam's ECT terminal has been leading in this respect with the introduction of an AGV and an ASC at the former Delta-Sealand Terminal in 1992. An automated transfer crane(ATC) control system is required with highest productivity. This tendency may also show the optimal way to solve the employment problems, the cost saving problems and the improvement of efficiency in port systems[1,2].

To consider nonlinear elements of an ATC, we are to design the controller for crane automatic position and anti-sway. PID controller has been widely used in actual industry because of its convenience and ordinary usage for user. As transfer crane has lots of dynamic characteristics, PID parameters must be changed in varying conditions automatically. An ATC can have controlled using Neural

Network(NN) that is one of robust intelligent control theory about nonlinearity[7,8,9].

In this paper, we would develop an ATC system with anti-sway above three techniques and construct proposed controller in on-line manner. The experimental results are shown that an ATC system controlled by the proposed controller has better driving performances and anti-sway than the others.

2. Automated Transfer Crane

2.1 Generalized coordinates of an ATC

Fig. 1 shows the coordinate system of an overhead crane and its load. In this paper, we assume that the considered overhead crane system is satisfied with the following conditions:

(1) A transfer crane supposes that do only plane moment, that is, the sway of container supposes that happen in plane made by transfer direction and container of trolley.
(2) The container has hanged down in rope that there is no mass.

The origin of the trolley coordinate system is $(x,y,0)$ the fixed coordinate system. Each axis of the trolley coordinate system is parallel to the counterpart of the fixed coordinate system and $\theta = (\theta_x, \theta_y)^T$.
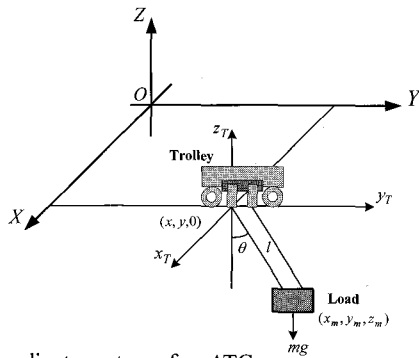

Fig. 1 Coordinate system of an ATC

Then, the position of the load in the fixed coordinate system is given by

$$x_m = x + l \sin\theta_x \cos\theta_y \tag{1}$$
$$y_m = y + l \sin\theta_y \tag{2}$$
$$z_m = -l \cos\theta_x \cos\theta_y \tag{3}$$

2.2 Motion equation of an ATC

In this section, the motion equations of an ATC system are derived using Lagrange's equation[3,4,5]. Especially, the load is considered as a point mass, and the mass and stiffness of the rope are also neglected. The kinetic energy of an ATC and its load K and the potential energy of the load P are given as follows:

$$K = \frac{1}{2}(M_x \dot{x}^2 + M_y \dot{y}^2 + M_l \dot{l}^2) + \frac{1}{2}mv_m^2 \tag{4}$$

$$P = mgl(1 - \cos\theta_x \cos\theta_y) \tag{5}$$

where

$$v_m^2 = \dot{x}_m^2 + \dot{y}_m^2 + \dot{z}_m^2$$
$$= \dot{x}^2 + \dot{y}^2 + \dot{l}^2 + l^2\dot{\theta}_x^2 \cos^2\theta_y + l^2\dot{\theta}_y^2$$
$$+ 2(\dot{l}\sin\theta_x \cos\theta_y + l\dot{\theta}_x \cos\theta_x \cos\theta_y - l\dot{\theta}_y \sin\theta_x \sin\theta_y)\dot{x}$$
$$+ 2(\dot{l}\sin\theta_y + l\dot{\theta}_y \cos\theta_y)\dot{y} \tag{6}$$

Also, Rayleigh's dissipation function is described as follows:

$$D = \frac{1}{2}(D_x \dot{x}^2 + D_y \dot{y}^2 + D_l \dot{l}^2) \tag{7}$$

For, small swing, we know the following conditions:

$$\sin\theta_x \approx \theta_x, \quad \sin\theta_y \approx \theta_y$$
$$\cos\theta_x \approx 1, \quad \cos\theta_y \approx 1 \tag{8}$$

In this case, the high order terms in the nonlinear model can be neglected with the trigonometric functions approximated. Then the nonlinear for an ATC system is simplified to be the linearized model as follows:

$$(M_x + m)\ddot{x} + ml\ddot{\theta}_x + D_x \dot{x} = f_x \tag{9}$$
$$(M_y + m)\ddot{y} + ml\ddot{\theta}_y + D_y \dot{y} = f_y \tag{10}$$
$$(M_l + m)\ddot{l} + D_l\ddot{l} - mg = f_l \tag{11}$$
$$l\ddot{\theta}_x + \ddot{x} + g\theta_x = 0 \tag{12}$$
$$l\ddot{\theta}_y + \ddot{y} + g\theta_y = 0 \tag{13}$$

In this crane system, the object to be controlled is the trolley position, the wire lope length, and the load swing angle. Also, this linearized dynamic model consists of the travel dynamics eqs. (9) and (12), the traverse dynamics eqs. (10) and (13), and the independent load hosting dynamic eq. (10).

3. Path Planning Method of an ATC System

3.1 Problem statement of path planning

In case that an ATC system transport containers in yard, it can be distributed into 5 actuation varieties as shown in Fig. 2. In this figure, the section AB exists an only perpendicular motion of hoist to B point and has the maximum perpendicular velocity, the section BC increases maximally when the velocity of trolley is 0. The other hand, the velocity of hoist decreases maximum to minimum. Also, a swing angle of an ATC system may be 0 at the point C as possible as one can. The swing angle in the section CD exists small and the maximum horizontal moving of trolley exists only. Finally, the section DC and EF have the reverse action between the section AB and BC, respectively.
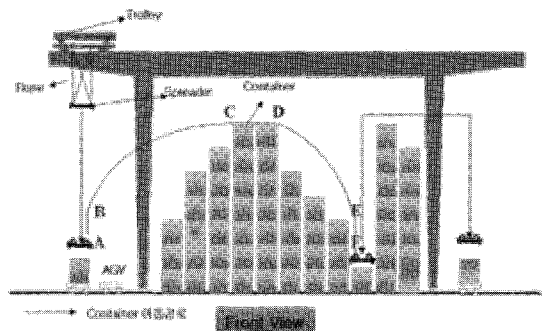

Fig. 2 Each transportation path of an ATC

In this paper, we shall propose the optimal path moving method in order to solving the path moving problem of trolley in an ATC system. Therefore the technique development for investigating the moving paths is required to many researches in order to improve work ability of an ATC system and prevent a loading container from collision in yard. To assign the optimal path for container moving in this research, we propose an effective search algorithm for collision avoidance path which connect both the incoming position A of containers and the outgoing position F and develop the tracking of assigned collision avoidance path and the predictive moving algorithm for transporting containers in the minimum time simultaneously[7,9].

3.2 A path search and minimum distance calculation for moving an ATC
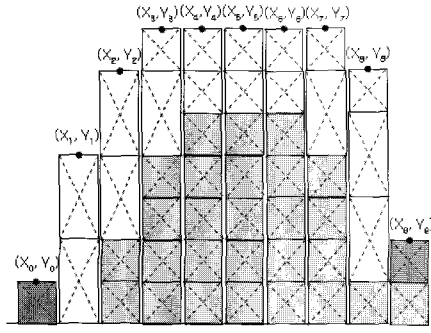
Fig. 3 An imaginary transportation path and an ATC profile

In this paper, the containers are divided into lattice format of a rectangular parallelepiped as size and configuration of theirs, and each unit-lattice is composed by the characteristic coordinates (X_i,Y_i) as shown in Fig. 3. To apply a yard map concept, the method for searching the path, which does not happen to collision between a carried container and various equipments, is summarized as follows:

(1) First, we must frame the yard map to indicate various avoidance distributions in yard. Therefore we use 2-dimensional lattices of a right-angle hexahedron in order to draw the yard map. Each lattice is used to specify proper addresses, i.e., the address (X_i,Y_i) is defined by the i-th address x_i on x-axis and the j-th address y_j on y-axis.

(2) To apply *configuration space technique*, which that the container is described as one point through the extension of container size for moving around a carrying container expressed in the yard map, we reframes the yard map into search space construction.

(3) We apply an optimal method for searching anti-collision path in yard space. In this paper, we select the optimal method for tracking the reference point based on experience information among available search methods.

To track the reference point effectively using *Best-first search method*, we first decide the evaluation function as follows:

$$F = \alpha_1 d_1 + \alpha_2 d_2 + \alpha_3 d_3 \tag{14}$$

Here, α_i $(i = 1,2,3)$ are weight values. In this paper, the coordinate point of container profile could be set as the following conditions;

(1) d_1 : It is defined by value that reflects the XY-plane upper from removable contiguity node t to goal node G.

$$d_1 = \sqrt{(x_G - x_t)^2 + (y_G - y_t)^2} \tag{15}$$

(2) d_2 : It is defined by the orthogonal distance to line segment that connects the start node S and the goal node G in contiguity node t projected XY-plane upper to altitude as follows:
$$ax + by + c = 0$$
$$a = y_G - y_S, \quad b = x_S - x_G \tag{16}$$
$$c = (x_G - x_S)y_S - (y_G - y_S)x_S$$
where the equation of straight line d_2 is given by

$$d_2 = \frac{|ax_t + by_t + c|}{\sqrt{a^2 + b^2 + c^2}} \tag{17}$$

(3) d_3 : The equation of straight line L_1 and L_2 is defined by

$$L_1 : \quad \frac{x - x_p}{l_1} = \frac{y - y_p}{m_1} = \frac{z - z_p}{n_1} = t_1$$

$$L_2 : \quad \frac{x - x_p}{l_2} = \frac{y - y_p}{m_2} = \frac{z - z_p}{n_2} = t_2 \tag{18}$$

where

$$l_1 = x_n - x_p, \quad l_2 = x_t - x_n$$
$$m_1 = y_n - y_p, \quad m_2 = y_t - y_n \tag{19}$$
$$n_1 = z_n - z_p, \quad n_2 = z_t - z_n$$

Then an angle d_3 is represented by

$$\cos d_3 = \frac{l_1 l_2 + m_1 m_2 + n_1 n_2}{\sqrt{l_1^2 + m_1^2 + n_1^2}\sqrt{l_2^2 + m_2^2 + n_2^2}} \tag{20}$$
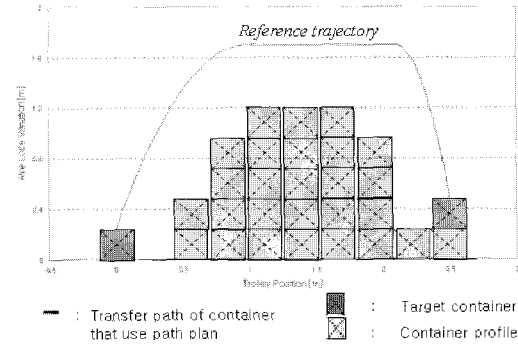

Fig. 4 The path search of reference trajectory for an ATC profile

Therefore, the anti-collision path express the knot point located in the conveyance path of container, and then each cross point also represents the reference point of unit-lattice as shown in Fig. 4.

The anti-collision path is specified by the selection of weight values α_1, α_2, and α_3 used in Eq. (14), then we can search for the value of evaluation function that can be optimal path. The terms d_1, d_2, and d_3 in Eq. (14) are to guarantee approachability for searching the goal node, to be not escape from straight line between start point and goal point, and to select that the variant of direction angle of straight line to be connected by the created nodes, respectively.

4. Design of NNP PID Controller

4.1 PID controller

In this paper, we will compose PID controller with 2 DOF that contains feedback type as shown in Fig. 5. This controller is very good effectiveness not only the estimation performance of fixing value but also the removal ability of disturbance. Therefore we study the problems to apply the position of an ATC and the anti-sway control of load.
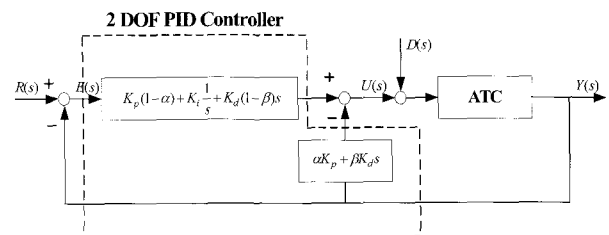

Fig. 5 PID controller with 2 DOF for an ATC

First, the controller output in Fig. 5 is described by

$$U(s) = E(s)\{K_p(1-\alpha) + \frac{K_i}{s} + (1-\beta)\}K_d s\}$$
$$- (\alpha K_p + \beta K_d s)Y(s)$$

(21)

where K_p, K_i, and K_d are gains of PID controller, respectively, the goal position and the swing angle of load is set by $Y(s)$, and the parameters α and β derive from the transformation of PID controller for various types. Moreover the necessary parameters for PID controller given by Eq. (21) is computed by NN auto tuning, and then the position error, length error of rope, and swing error are composed by the estimations of 15 parameters, respectively. The disturbance $D(s)$ is also considered by a strong wind of regular period at all times as follows:

$$F_\omega = p(3\sin \omega t + 7\sin 2\omega t + 5\sin 3\omega t + 4\sin 4\omega t)$$

(22)

where ω is fundamental frequency of wind and p is wind magnitude.

4.2 NN modeling and predictive system

NNP system is composed of predictive system based on the present input/out information which is learned by executing the modeling learning about plant. The block diagram of neural network modeling learning and the proposed structure of 2-step NNP are shown in Fig. 6 and Fig. 7, respectively.
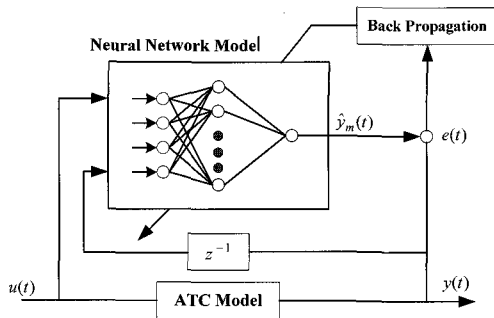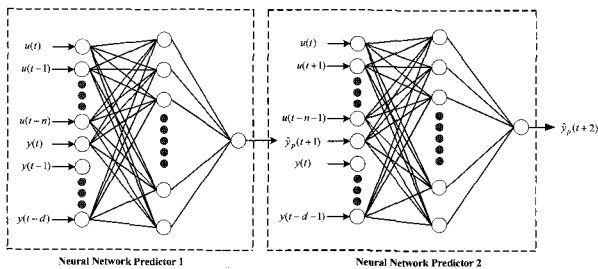

Fig. 6 Modeling of neural network

Fig. 7 Structure of neural network predictor

In Fig. 7, the control parameter is the position and angle of trolley. Also, the predictive output get using two NN predictors and the structure consists of 2-step predictor

4.3 NN predictive PID controller

we will propose the design results for PID controller to have ability to eliminate the disturbance and the performance to pursuer a target in order to control the stacking an ATC system. The proposed NNP PID control system is shown in Fig. 8. In this figure, the system configuration is composed of 3 parts; i) Neural network predictor, ii) Neural network auto tuner, iii) PID controller. Neural network predictor can estimate the future output from the input information of current input/output of plant, and then NN auto tuner in order to

compensate errors between the calculated predictive output and current output of plant computers parameters of controller through on-line learning scheme. Also, we used PID controller used to an industrial fields widely.
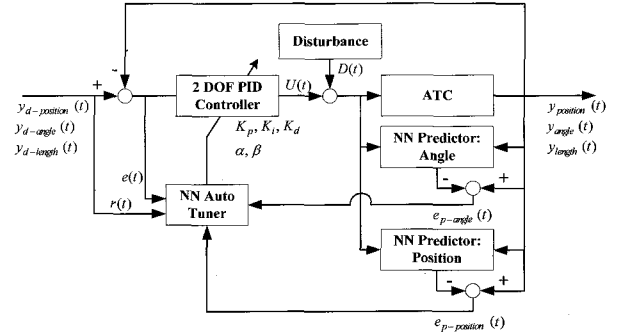

Fig. 8 Block diagram of NNP PID controller

In general, PID controller is known that this controller to have a simple structure is easily realized by linear controller and should be ensure robustness certainly, however the actuate point of control system to require adaptiveness can not be sufficient control performances.
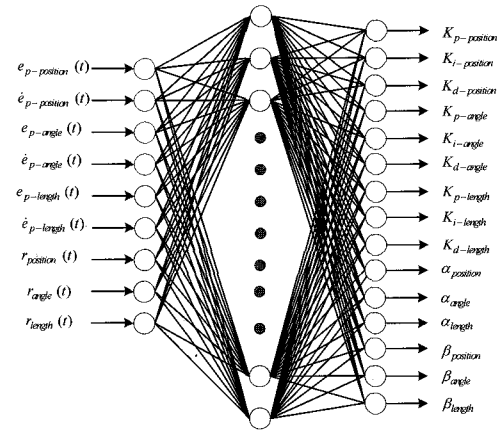

Fig. 9 Neural network self-tuner

To overcome this problem, we will compute parameters of PID controller using NN auto tuner and the structure of NN auto tuner is shown in Fig. 9. Here, we use the momentum back propagation learning method and the input layer vector is composed of the error, the deviation of error, the predictive position of trolley, and an angle output and desired value. The activation functions of both hidden and output layers are sigmoid and linear function, respectively.

Here, we used NN algorithm to tune the parameters of PID control in online manners. The discrete time version of input of NNP PID controller is represented as follows:

$$u(t) = \{(1-\alpha_p)k_{p\_p}(e_p(t) - e_p(t-1)) + k_{i\_p}e_p(t)$$
$$+ (1-\beta_p)k_{d\_p}(e_p(t) - 2e_p(t-1) + e_p(t-2))\}$$
$$+ \{(1-\alpha_a)k_{p\_a}(e_a(t) - e_a(t-1)) + k_{i\_a}e_a(t)$$
$$+ (1-\beta_a)k_{d\_a}(e_a(t) - 2e_a(t-1) + e_a(t-2))\}$$
$$+ \{(1-\alpha_l)k_{p\_l}(e_l(t) - e_l(t-1)) + k_{i\_l}e_l(t)$$
$$+ (1-\beta_l)k_{d\_l}(e_l(t) - 2e_l(t-1) + e_l(t-2))\}$$
$$- \{\alpha_p k_{p\_p}(y_p(t) - y_p(t-1))$$
$$+ \beta_p k_{d\_p}(y_p(t) - 2y_p(t-1) + y_p(t-2))\}$$
$$- \{\alpha_a k_{p\_a}(y_a(t) - y_a(t-1))$$
$$+ \beta_a k_{d\_a}(y_a(t) - 2y_a(t-1) + y_a(t-2))\}$$
$$- \{\alpha_l k_{p\_l}(y_l(t) - y_l(t-1))$$
$$+ \beta_l k_{d\_l}(y_l(t) - 2y_l(t-1) + y_l(t-2))\}$$

(23)

where $e(t) = [e_p(t) \quad e_a(t) \quad e_l(t)]^T$ and the parameters given by Eq. (22) are shortly described as the subscripts of parameters shown in Fig. 9. Note that $e_{p-position}(t)$, $e_{p-angle}(t)$ and $e_{p-length}(t)$ are expressed by $e_p(t)$, $e_a(t)$ and $e_l(t)$, respectively.

Also, the disturbance is used in Eq. (22) and the estimation function is used error function using eq. (24). Also, Error function E in eq. (24) can be minimized by adjusting weight values. Note that it finds minimum of error function by the gradient descent. Based on the gradient descent method, both output layer and hidden layer are described by:

$$E = \frac{1}{2}[y_{d-position}(t) - x(t)]^2$$

$$E = \frac{1}{2}[\theta_{d-angle}(t) - \theta(t)]^2 \tag{24}$$

$$E = \frac{1}{2}[y_{d-length}(t) - y(t)]^2$$

$$\Delta W_{jk}(t) = -\eta \frac{\partial E}{\partial W_{jk}} + \varepsilon \Delta W_{jk}(t-1)$$

$$\Delta W_{ij}(t) = -\eta \frac{\partial E}{\partial W_{ij}} + \varepsilon \Delta W_{ij}(t-1) \tag{25}$$

where η and ε are the learning rate and momentum constant, respectively.

Then the error signal of output layer is given by

$$\delta_k = -\frac{\partial E}{\partial net_k}$$

$$= -\frac{\partial E}{\partial y(t+1)} \frac{\partial y(t+1)}{\partial u(t)} \frac{\partial u(t)}{O(k)} \frac{\partial O(k)}{\partial net_k} \tag{26}$$

where

$$net_k = \sum_j W_{jk} O_j + \theta_k \tag{27}$$

$$o_{pj}(k) = f_j(net_{pj}) = f_j(\sum_j w_{ji} o_j) \tag{28}$$

Using the chain rule, the update weights between hidden layer and output layer is calculated by:

$$\Delta W_{jk}(t+1) = \eta \delta_k O_j + \varepsilon \Delta W_{jk}(t) \tag{29}$$

5. Experiment

5.1 Configuration of an ATC system

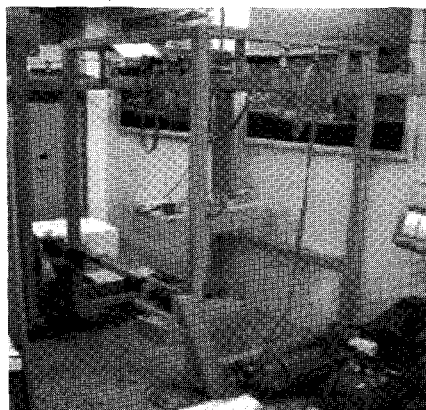The structure of an ATC simulator manufactured in this paper is shown in Fig. 10.

Fig. 10 Structure of an ATC simulator system

The magnitude of an ATC simulator and the volume of a container are $W\,3580 \times D\,540mm \times H\,1640mm$ and $W\,600 \times D\,240 \times H\,130mm$, respectively. Moreover the schematic diagram for experiment is also shown in Fig. 11 and the manufactured ATC system is composed of four parts; i) control part, ii) driving part, iii) communication part, and iv) sensor part. In this system, since the information of driving error is transmitted to DSP through RS232 communication, it can be exchanged with the information for driving controller and composed of generating the driving signals of each motor by receiving encoder datum such as control algorithm in DSP, the distance and position between trolley and hoist of an ATC system, etc.

As we observe the motion process of automatic driving control for an ATC system shown in Fig. 11, we estimate an anti-sway angle and position using potentiometer and encoder, respectively. Furthermore we can compute a control input form the estimate value to be inputted from PC, and then the velocity command of motor is given by the control input calculated through DSP.
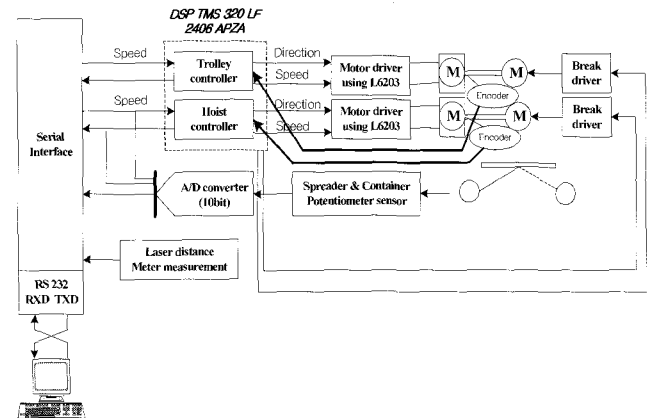

Fig. 11 Schematic diagram of an ATC system

5.2 Learning and test of NN model

NN tuner shown in Fig. 9 is tuned by eq. (23) on the one step and by online. However the tuner was tuned enough to satisfy the following condition without the actual plant by using NN models in order to avoid an initial damage at the tuner applying. The parameters of NN tuner such as weights were memorized whenever simulations and experiments were performed. Then the parameters of NN tuner are also specified as follows:

· Hidden layer size: 38
· No. delayed plant inputs: 3
· No. delayed plant output: 8
· Training samples: 10,000
· Epochs: 50

NN learning samples and its results of identification of angle and position model are shown as Fig. 12 and Fig. 13, respectively. In the case of NN model for the position of trolley used the learning, the learning is not performed well.
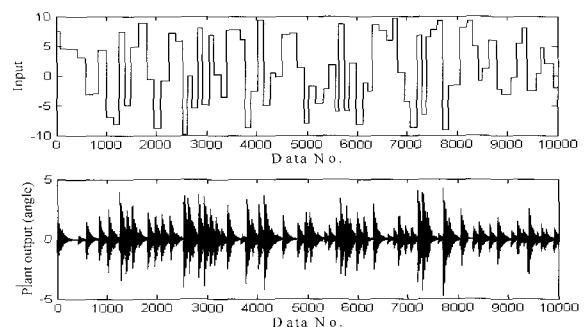

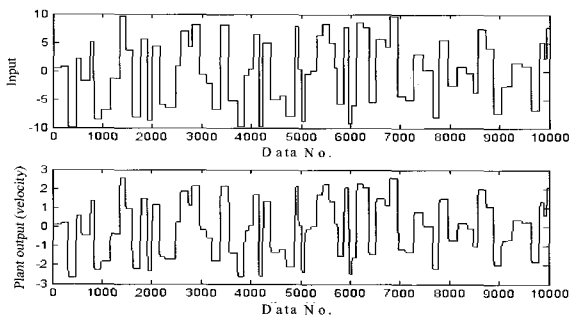Fig. 12 Training data for NN angle model

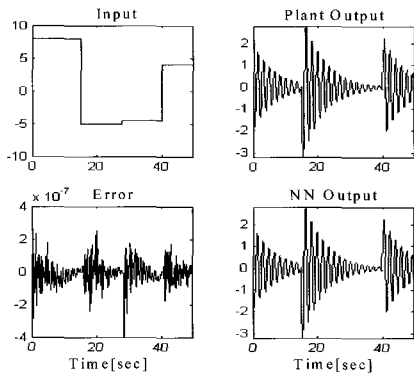Fig. 13 Training data for NN position model

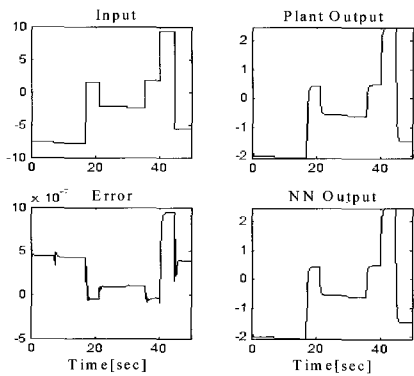Fig. 14 Test result of NN angle model

Fig. 15 Test result of NN position model

Therefore the position of NN model is learned by trolley speed with integrator. Furthermore the test results for both of NN models are shown as Fig. 14 and Fig. 15, respectively. Errors between the model and plant are less than 10^{-6}.

5.3 Experimental results

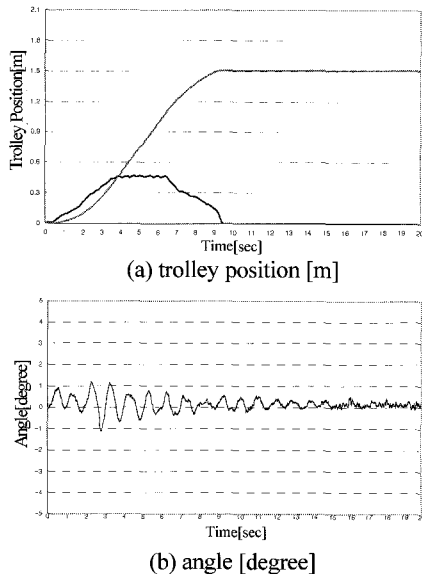(a) trolley position [m]

(b) angle [degree]

Fig. 16 Response characteristic of PID control

Fig. 16 and Fig. 17 show the experimental results with response characteristics of PID and NNP PID controllers when the weight of container for an ATC is 10[kg]. Here, when the final target position and the initial angle of an ATC set up 1.5[m] and 0[degree], respectively, we experiment on the estimate state to the target position 1.5[m] of trolley.

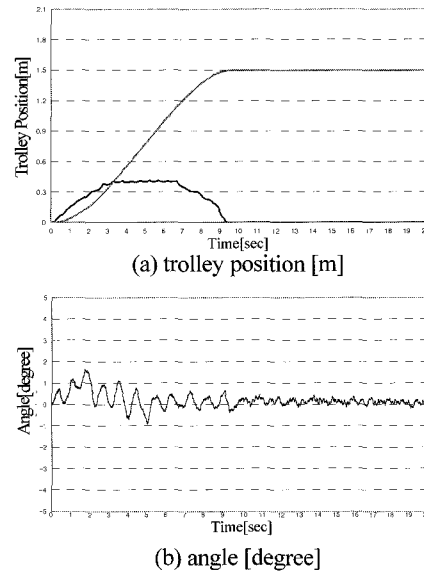(a) trolley position [m]

(b) angle [degree]

Fig. 17 Response characteristic of NNP PID control

Furthermore, we show the response characteristics of PID and NNP PID controllers as shown in Fig. 18 and Fig. 19. In these figures, the weight of container increases about 15[kg] and the disturbance is also added by an initial state of disturbance.

(a) trolley position [m]
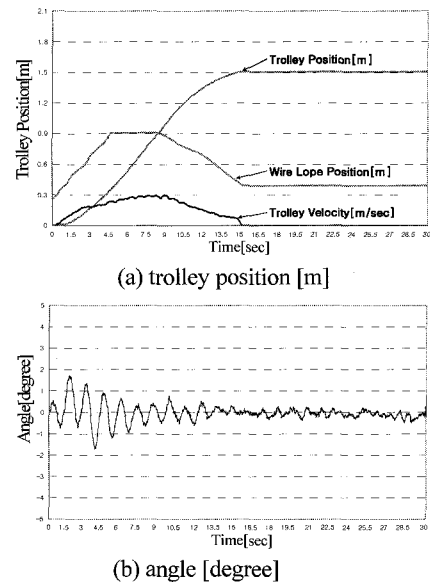

(b) angle [degree]

Fig. 18 Response characteristic of PID control

Moreover, the main characteristics of each item for PID and NNP PID controllers with a wind force are compared with Table 1, respectively. Compared with each term, we know that swing angle of NNP PID controller decreases more 0.1862[degree] than PID controller and the amplitude of swing angle also decreases more 0.049[degree] than PID controller.
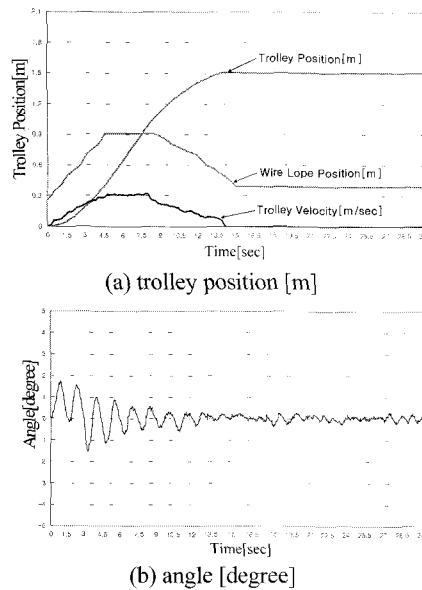
(a) trolley position [m]

(b) angle [degree]

Fig. 19 Response characteristic of NNP PID control

Table 1 Comparison of performances between PID control and NNP PID control

Response characteristics	PID	NNP PID
Position settling time [sec]	14.95	14.20
Position error [m]	0.005785	0.004992
Swing angle [degree]	-1.6704 ~ 1.7302	-1.4896 ~ 1.7248
Amplitude of swing angle [degree]	-0.3376 ~ 0.2994	-0.3430 ~ 0.2450

6. Conclusions

In this paper, we develop anti-sway control in proposed techniques for an ATC system. First, the developed algorithm is to build the optimal path of container motion and to calculate an anti-collision path for collision avoidance in its movement to the finial coordinate.

In order to show the effectiveness in this research, we compared NNP PID controller to be tuning parameters of controller using NN with 2-DOF PID controller. The experimental results show that the proposed control scheme guarantees good performances, trolley position, sway angle, and settling time in NNP PID controller than other controller. By using the proposed controller, there were improvements of 4.7% and 13.6% for settling time and trolley position error than the conventional PID controller respectively. Moreover, the sway angle could be reduced to 5.5% by NNP PID controller. We researched about develop of the ATCS in the techniques for unmanned automation of the ATC. Besides, we designed the NNP PID controller using the NN predictor, and compared with the conventional controller. As result, the application of NNP PID controller is analyzed to have robustness about disturbance which is wind of fixed pattern in the yard. Accordingly, the proposed algorithm proposed in this study can be readily used for industrial applications.

In the further works, we should execute the proposed control algorithm for the similar size of an actual ATC system in order to overcome the limits of simulator system. Also, we must consider AC motor used in ATC system instead of DC servo motor in the actual experiments.

REFERENCES

1. Sakawa, Y. and Shindo Y., "Optimal Control Container Crane," Trans. on IFAC, Vol. 18, No. 3, pp. 257-266, 1982.

2. Werbos, P. J., "Neural Networks and Human Mind: New mathematics fits humanistics insight," IEEE Trans. on Systems, Man, and Cybernetics, Vol. 1, pp. 78-83, 1992.

3. Lee, J. K, Park, Y. J. and Lee, S. R., "Development of a Motion Control Algorithm for the Automatic Operation System of Overhead Cranes," Trans. of the Korean Society of Mechanical Engineers, Vol. 20, No. 10, pp. 3160-3172, 1996.

4. Lee, H. H., "Modeling and Control of a Three-Dimensional Overhead Crane," ASME Journal of Dynamics Systems, Measurement and Control, Vol. 120, No. 4, pp. 471-476, 1998.

5. Tag, Y., Su, C. Y. and Cauwenberghe, A. V., "Neural Network based Smith Predictive Control for Nonlinear Process with Time-delay," Proc. of Asian Control Conference, pp. 315-320, 2000.

6. Kim, Y. B., "A Study on the Sway Control of a Crane Based on Gain-Scheduling Approach," Journal of the Korean Society of Precision Engineering, Vol. 18, No. 7, pp. 53-64, 2001.

7. Sohn, D. S., Lee, J. W., Lee, Y. J. and Lee, K. S., "A Study on Development of ATCS of Transfer Crane using Neural Network Predictive Control," Journal of Korean Navigation and Port Research, Vol. 26, No. 5 pp. 537-542, 2002.

8. Lee, T. Y., Lee, S. R., "Anti-sway and Position 3D Control of the Nonlinear Crane System using Fuzzy Algorithm," International Journal of Precision Engineering and Manufacturing, Vol. 3, No. 1, pp. 66-75, 2002.

9. Sohn, D. S., Lee, J. T., Lee, J. W., Lee, J. M. and Lee, K. W., "A Study on Development of ATCS for Automated Transfer Crane using Neural Network Predictive PID Controller," Proc. of SICE Annual Conference, pp. 3170-3175, 2003.

10. Lee, Y. J., Suh, J. H. and Lee, K. S., "A Study on Driving Control of an Autonomous Guided Vehicle using Humoral Immune Algorithm Adaptive PID Controller based on Neural Network Identifier Technique," Journal of the Korea Society of Precision Engineering, Vol. 21, No. 10, pp. 65-77, 2004.

11. Suh, J. H., Lee, J. W., Lee, Y. J. and Lee, K. S., "An Automatic Travel Control of a Container Crane using Neural Network Predictive PID Control Technique," Journal of the Korea Society of Precision Engineering, Vol. 22, No. 1, pp. 61-72, 2005.